# Reconstruction of parameters and unobserved variables of a semiconductor laser with optical feedback from intensity time series

I. V. Sysoev,[1,2] V. I. Ponomarenko,[1,2] B. P. Bezruchko,[1,2] and M. D. Prokhorov[1]

[1]*Saratov Branch of Kotelnikov Institute of Radioengineering and Electronics of Russian Academy of Sciences, Zelyonaya Street, 38, Saratov 410019, Russia*

[2]*Saratov State University, Astrakhanskaya Street, 83, Saratov, 410012, Russia*

(Received 14 February 2020; revised manuscript received 30 March 2020; accepted 9 April 2020; published 29 April 2020)

We propose a method for the reconstruction of time-delayed feedback systems having unobserved variables from scalar time series. The method is based on the modified initial condition approach, which allows one to significantly reduce the number of starting guesses for an unobserved variable with a time delay. The proposed method is applied to the reconstruction of the Lang-Kobayashi equations, which describe the dynamics of a single-mode semiconductor laser with external optical feedback. We consider the case where only the time series of laser intensity is observable and the other two variables of the model are hidden. The dependence of the quality of the system reconstruction on the accuracy of assignment of starting guesses for unobserved variables and unknown laser parameters is studied. The method could be used for testing the security of information transmission in laser-based chaotic communication systems.

DOI: 10.1103/PhysRevE.101.042218

## I. INTRODUCTION

The problem of reconstructing mathematical models of dynamical systems from time series has a long history [1–3]. As the dimension of the system increases, the reconstruction of its equations becomes more difficult. For example, for systems with time-delayed feedback, having an infinite-dimensional phase space, a direct reconstruction using conventional time-delay embedding techniques often fails. For a successful recovery of the time-delay systems, one has to use special methods [4–21]. These methods allow one to reconstruct parameters of time-delay systems using regression analysis [4,5], information-theory approaches [6,7], projection of the system phase space onto low-dimensional subspaces [8–12], analysis of extrema in the time series [13,14], multiple shooting approach [15], nearest neighbor analysis [16], synchronization [17,18], and other approaches [19–21]. There are also methods of time-delayed feedback system reconstruction based on the analysis of a system's response to external perturbations [22–25]. The problem of time-delay system recovery becomes more complicated if a time-delay system has hidden variables that are inaccessible for observation. At the same time, such a task is of practical interest, since the reconstruction of a mathematical model can be used as a method for indirect measurement of unobserved variables in this case.

In the present paper, we propose a method for the reconstruction of a time-delayed feedback system, in which only one of the three dynamical variables is observable and the other two variables are hidden, including a hidden variable with a time delay. The method is applied to the reconstruction of the Lang-Kobayashi equations [26], which describe the dynamics of a single-mode semiconductor laser with external optical feedback. In dimensionless form, the Lang-Kobayashi equations are written as follows:

$$\begin{aligned}\dot{\rho}(t) &= F(t)\rho(t)+\eta\rho(t-\tau)\cos[\phi(t)-\phi(t-\tau)+\Omega\tau],\\ \rho(t)\dot{\phi}(t) &= \alpha F(t)\rho(t)-\eta\rho(t-\tau)\sin[\phi(t)-\phi(t-\tau)+\Omega\tau],\\ T\dot{F}(t) &= P-F(t)-[1+2F(t)]\rho^2(t),\end{aligned} \tag{1}$$

where $\rho(t)$ and $\phi(t)$ are the modulus and phase of the complex electric field $E(t)=\rho(t)\exp[i\phi(t)]$, respectively; the time $t$ is normalized to the cavity photon lifetime $\tau_p(\sim 1\ \mathrm{ps})$; $F(t)$ is the excess carrier number; $T$ is the ratio of the carrier lifetime to the photon lifetime; $P$ is the dimensionless pumping current above threshold; $\tau$ is the ratio of the external cavity round-trip time and the photon lifetime; $\eta$ is the strength of the feedback; $\alpha$ is the linewidth enhancement factor; and $\Omega$ is the dimensionless angular frequency of the solitary laser [27,28]. $\Omega\tau$ is called the feedback phase and represents a constant phase shift incurred by the feedback field with respect to the laser field.

Semiconductor lasers described by the Lang-Kobayashi equations have been widely studied under change of model parameters [28–33]. These lasers are of particular interest, since they can generate wideband chaotic oscillations of very high dimension [34] and can be used for chaos-based secure optical communication [35–37]. The security of laser-based communication systems is explained mainly by the difficulty for an eavesdropper to recover the transmitter parameters from a transmitted chaotic signal.

A number of methods have been proposed for estimating the parameters of a semiconductor laser with optical feedback from time series [38–43]. Most of these methods are intended for the recovery of delay time in the optical feedback. For example, the delay time $\tau$ can be approximately estimated using the autocorrelation function [39,42] or delayed mutual

 

information calculated from time series of laser intensity $I(t) = |E(t)|^2 = \rho^2(t)$ [39]. However, these methods often give an overestimation of $\tau$. For more accurate reconstruction of $\tau$, one can use either the method based on the statistical analysis of extrema in the intensity time series [38] or the method based on the nearest neighbor analysis [43]. The problem of estimating the other laser parameters is much less studied.

Since the parameters $T$ and $\alpha$ are fixed in a real laser and take close values for lasers of the same type, we assume them to be known as well as the parameters $\tau$ and $\Omega$. We consider a typical situation for a physical experiment, in which only the time series of laser intensity is observable, and the phase $\phi(t)$ of the electric field and the excess carrier number $F(t)$ are hidden variables. The problem of reconstructing unobserved variables of the Lang-Kobayashi equations (1) has not yet been studied. The control parameters $P$ and $\eta$, which can be easily varied in the laser, are assumed to be unknown. Our goal is to reconstruct the parameters $P$ and $\eta$ and unobserved variables $\phi(t)$ and $F(t)$ from the intensity time series of the model (1).

A similar problem was considered recently in Ref. [44], in which a reservoir computing based algorithm was used for reconstructing two unobserved dynamical variables from a time series of only one observed dynamical variable. This algorithm was successfully applied to reconstruct the model of an optically injected class B semiconductor laser, which is described by the same three variables as the model (1), but these variables do not have any time delay. In contrast to our approach, the unobserved variables were reconstructed in Ref. [44] for a simpler case, in which all laser parameters are assumed to be known. Moreover, the reservoir computing method needs all three dynamical variables to be available for a limited period of time for training the algorithm. Our approach has no such limitations.

The paper is organized as follows. Section II contains the method description. Using the proposed method, in Sec. III, we recover the parameters and unobserved variables of the Lang-Kobayashi equations from periodic, chaotic, and intermittent time series of laser intensity. In Sec. IV we summarize our results.

## II. METHOD DESCRIPTION

In experimental studies of laser dynamics, the time series of laser intensity $I(t) = \rho^2(t)$ is usually available for observation and recording. Since $\rho(t) > 0$ by definition, its time series can be easily calculated from time series of $I(t)$ as $\rho(t) = \sqrt{I(t)}$. Let us assume that we have the time series $\{\rho_n\}_{n=1}^{N}$ of the variable $\rho(t)$ generated by Eq. (1), where $n = t/\Delta t$ is the discrete time, $\Delta t$ is the sampling time, and $N$ is the total number of samples. For convenience, we introduce the discrete delay time $\theta = \tau/\Delta t$.

Almost all methods dealing with the recovery of hidden variables are based on the initial condition approach [1]. Its main idea is to consider the initial conditions for hidden variables as additional unknown parameters of the model equations. Then, starting guesses (initial values) are specified for all unknown parameters. At the next step, the objective function is introduced, which depends on the model parameters and characterizes the distances between the points of the model time series and observed time series. By minimizing the objective function, one can reconstruct both the model parameters and unobserved variables. Such approach and its modified variants [45,46], known as the multiple shooting approach, have been successfully applied for the reconstruction of systems described by ordinary differential equations [47,48].

If one of the hidden variables, for example, the variable $\phi(t)$ in Eq. (1), has a time delay, it is necessary to specify $(\theta + 1)$ starting guesses for this variable. However, the straightforward application of the initial condition approach to time-delay systems in most cases does not lead to success [49]. Only simple periodic regimes and only in the case of small delay times ($\theta \leqslant 11$) can be reconstructed using such technique. It is explained by the fact that the number of the objective function parameters increases with the increase of $\theta$. As a result, the problem of global optimization of the objective function becomes more difficult, because the basin of attraction of the global minimum becomes smaller.

To overcome this shortcoming of the method, we take into account the fact that the arguments of the objective function are not completely independent, since the neighbor points of a trajectory of a time-delayed hidden variable should be strongly correlated. In the case of large delay time, one can specify only a small portion of the initial conditions for $\phi(t)$, specifying them only for the points of $\phi(t)$ located far away in time one from another. However, to simulate the time series of Eq. (1), it is necessary to have all $(\theta + 1)$ starting guesses for the hidden variable. We propose to use cubic spline interpolation for obtaining all intermediate values of initial conditions for $\phi(t)$.

Let us define the starting guesses for the unobserved variables $\phi(t)$ and $F(t)$ as $\{\tilde{\phi}_n\}_{n=1}^{\theta+1}$ and $\tilde{F}_{\theta+1}$, respectively, and the starting guesses for the unknown parameters $P$ and $\eta$ as $\tilde{P}$ and $\tilde{\eta}$, respectively. The other parameters of Eq. (1) are assumed to be known. All together, the starting guesses can be written as a vector

$$\boldsymbol{\zeta} = (\tilde{\phi}_1, \ldots, \tilde{\phi}_\theta, \tilde{\phi}_{\theta+1}, \tilde{F}_{\theta+1}, \tilde{P}, \tilde{\eta}). \tag{2}$$

Instead of specifying $(\theta + 1)$ values of $\tilde{\phi}_n$, we specify only $L$ ($L \ll \theta$) $\tilde{\phi}_n$ values, where $n = n_1, \ldots, n_L$ with $n_1 = 1$ and $n_L = \theta + 1$. This approach allows us to significantly reduce the number of starting guesses for the unobserved variable $\phi(t)$. In general, the instants of time $n_i$ are not necessary equidistant. However, for convenience, we use equidistant starting guesses $\tilde{\phi}_{n_i}$ with $n_i = 1 + [\frac{(i-1)\theta}{L-1}]$, where $i = 2, \ldots, L-1$ and square brackets denote the integer part of a number. As a result, the vector (2) can be rewritten as follows:

$$\boldsymbol{\zeta} = \left(\tilde{\phi}_{n_1}, \ldots, \tilde{\phi}_{n_L}, \tilde{F}_{\theta+1}, \tilde{P}, \tilde{\eta}\right). \tag{3}$$

The vector (3) consists of $K$ components, which we denote as $\zeta_1, \ldots, \zeta_K$. We specify the vector (3) and calculate $(\theta + 1 - L)$ intermediate $\tilde{\phi}_n$ values using cubic spline approximation. Then, we generate the model time series $\{\hat{\rho}_n\}_{n=\theta+2}^{N}$ by solving Eq. (1) with the observed $\{\rho_n\}_{n=1}^{\theta+1}$ values as initial conditions for $\rho(t)$. The objective function can be calculated

as follows:

$$S(\boldsymbol{\zeta}) = S(\zeta_1, \ldots, \zeta_K) = \sum_{n=\theta+2}^{N} (\rho_n - \hat{\rho}_n)^2. \tag{4}$$

The function (4) characterizes the sum of squares of the distances between the points of the observed time series and model time series. To minimize the function $S$, we can use one of the classical optimization techniques. In the present paper, the minimization of $S$ is carried out using the gradient descent algorithm, which requires the calculation of the gradient,

$$\mathbf{g} = \left( \frac{\partial S}{\partial \zeta_1}, \ldots, \frac{\partial S}{\partial \zeta_K} \right), \tag{5}$$

and the Hessian matrix,

$$\mathbf{H} = \begin{bmatrix} \frac{\partial^2 S}{\partial \zeta_1^2} & \frac{\partial^2 S}{\partial \zeta_1 \partial \zeta_2} & \cdots & \frac{\partial^2 S}{\partial \zeta_1 \partial \zeta_K} \\ \frac{\partial^2 S}{\partial \zeta_2 \partial \zeta_1} & \frac{\partial^2 S}{\partial \zeta_2^2} & \cdots & \frac{\partial^2 S}{\partial \zeta_2 \partial \zeta_K} \\ \vdots & \vdots & \ddots & \vdots \\ \frac{\partial^2 S}{\partial \zeta_K \partial \zeta_1} & \frac{\partial^2 S}{\partial \zeta_K \partial \zeta_2} & \cdots & \frac{\partial^2 S}{\partial \zeta_K^2} \end{bmatrix}. \tag{6}$$

The direct analytic or asymptotic calculation of $\mathbf{g}$ and $\mathbf{H}$ is not possible, since explicit dependence of the objective function $S$ on its arguments is not known and cannot be expressed explicitly for most types of oscillation regimes. However, $\mathbf{g}$ and $\mathbf{H}$ can be estimated numerically. We add a small perturbation $\pm\delta\zeta_i$ sequentially to each $i$th component $\zeta_i$ of the vector $\boldsymbol{\zeta}$ and generate the perturbed time series by solving Eq. (1). Then, the $i$th component $g_i$ of the gradient (5) can be estimated using the following approximate formula:

$$g_i \approx \frac{S(\zeta_1, \ldots, \zeta_i + \delta\zeta_i, \ldots, \zeta_K) - S(\zeta_1, \ldots, \zeta_i - \delta\zeta_i, \ldots, \zeta_K)}{2\delta\zeta_i}. \tag{7}$$

In a similar way, each component $h_{i,j}$ of the Hessian matrix can be numerically estimated by sequentially introducing perturbations simultaneously to the two components ($\zeta_i$ and $\zeta_j$) of the vector $\boldsymbol{\zeta}$:

$$\begin{aligned} h_{i,j} &\approx \frac{S_{i+j+} - S_{i+j-} - S_{i-j+} + S_{i-j-}}{4\delta\zeta_i\delta\zeta_j}, \\ S_{i+j+} &= S(\zeta_1, \ldots, \zeta_i + \delta\zeta_i, \ldots, \zeta_j + \delta\zeta_j, \ldots, \zeta_K), \\ S_{i+j-} &= S(\zeta_1, \ldots, \zeta_i + \delta\zeta_i, \ldots, \zeta_j - \delta\zeta_j, \ldots, \zeta_K), \\ S_{i-j+} &= S(\zeta_1, \ldots, \zeta_i - \delta\zeta_i, \ldots, \zeta_j + \delta\zeta_j, \ldots, \zeta_K), \\ S_{i-j-} &= S(\zeta_1, \ldots, \zeta_i - \delta\zeta_i, \ldots, \zeta_j - \delta\zeta_j, \ldots, \zeta_K). \end{aligned} \tag{8}$$

Having the gradient of the objective function and the Hessian matrix, we can calculate the vector of corrections $\boldsymbol{\Delta\zeta}$ to the starting guesses $\boldsymbol{\zeta}$ by solving the system of linear equations,

$$\mathbf{H}\boldsymbol{\Delta\zeta} = -\mathbf{g}. \tag{9}$$

Since the gradient method often gives corrections that are too large, we check the condition,

$$S(\boldsymbol{\zeta} + \boldsymbol{\Delta\zeta}) < S(\boldsymbol{\zeta}). \tag{10}$$

If the inequality (10) does not hold, then we reduce the correction $\boldsymbol{\Delta\zeta}$ by half. This check is repeated up to 20 times. If, even after this multiple check, the inequality (10) does not hold, then the algorithm stops. If the inequality (10) holds, then we adjust the vector of starting guesses $\boldsymbol{\zeta}$ by adding a vector of corrections $\boldsymbol{\Delta\zeta}$ to it, and again calculate the objective function. This procedure is repeated until the change in the objective function at the next step of algorithm becomes sufficiently small:

$$S(\boldsymbol{\zeta}) - S(\boldsymbol{\zeta} + \boldsymbol{\Delta\zeta}) < \varepsilon, \tag{11}$$

where the parameter $\varepsilon$ sets the accuracy of calculations. We set $\varepsilon = 10^{-10}$ throughout the paper.

Similarly to other methods of optimization, the gradient descent algorithm often finds a local minimum, but not the global one. Hence, the results of the proposed approach depend on the choice of starting guesses for both laser parameters and unobserved variables. To achieve good accuracy of the parameters $P$ and $\eta$ reconstruction, we vary their starting guesses $\tilde{P}$ and $\tilde{\eta}$ in the two-dimensional space with the steps $\Delta P$ and $\Delta\eta$, respectively. Note that it is possible to reduce the investigated part of the parameter plane $(\tilde{P}, \tilde{\eta})$ by using the charts of dynamical regimes [28] for detecting the ranges of $P$ and $\eta$ values, at which the observed regime of oscillations can take place. The oscillation regime can be easily defined from the observable time series of $I(t)$. Since we know the oscillation regime, we limit the interval for changing the starting guesses $\tilde{F}_{\theta+1}$ for the hidden variable $F(t)$ by the values at which the observed regime can be realized. Then, we vary $\tilde{F}_{\theta+1}$ in this interval with a certain step. Hence, the appropriate starting guesses for the parameters $P$ and $\eta$ and the variable $F(t)$ should be searched in a three-dimensional space.

Since we use a cubic spline for interpolating the initial conditions for the time-delayed hidden variable $\phi(t)$ on the delay time interval, it is necessary to specify at least three starting guesses $\tilde{\phi}_n$. As a result, the dimension of the parameter space greatly increases and the method of reconstruction fails, because it needs too much computation time for scanning the high-dimensional parameter space. Therefore, we have to use another approach taking into account that for the considered regimes, the characteristic period of oscillations is much greater than the delay time $\tau$. We propose to specify the starting guesses for $\phi(t)$ using the linear approximation

$$\tilde{\phi}(t) = \tilde{\omega}t + \tilde{\varphi}, \tag{12}$$

where $\tilde{\omega}$ characterizes the straight line slope and $\tilde{\varphi}$ defines the initial value of $\phi(t)$. We do not search for $\tilde{\omega}$ and $\tilde{\varphi}$ values corresponding to the global minimum of the objective function. Instead, we vary $\tilde{\omega}$ in the range $[-10/\tau, 10/\tau]$ with the step $0.5/\tau$ and $\tilde{\varphi}$ in the range $[-5, 5]$ with step 1. Some combinations of $\tilde{\omega}$ and $\tilde{\varphi}$ provided good enough quality of reconstruction for the chosen $\tilde{P}$, $\tilde{\eta}$, and $\tilde{F}_{\theta+1}$.

## III. METHOD APPLICATION

To test the proposed technique, we consider the laser regimes with the parameters $T = 1710$, $\alpha = 5$, $\Omega = -0.1962$, $P = 0.6$, and $\eta = 0.015$ taken from Refs. [27,28]. Three qualitatively different regimes of oscillations are observed under variation of the delay time $\tau$. Figure 1 shows the time series of $\rho(t)$ in system (1) at sampling time

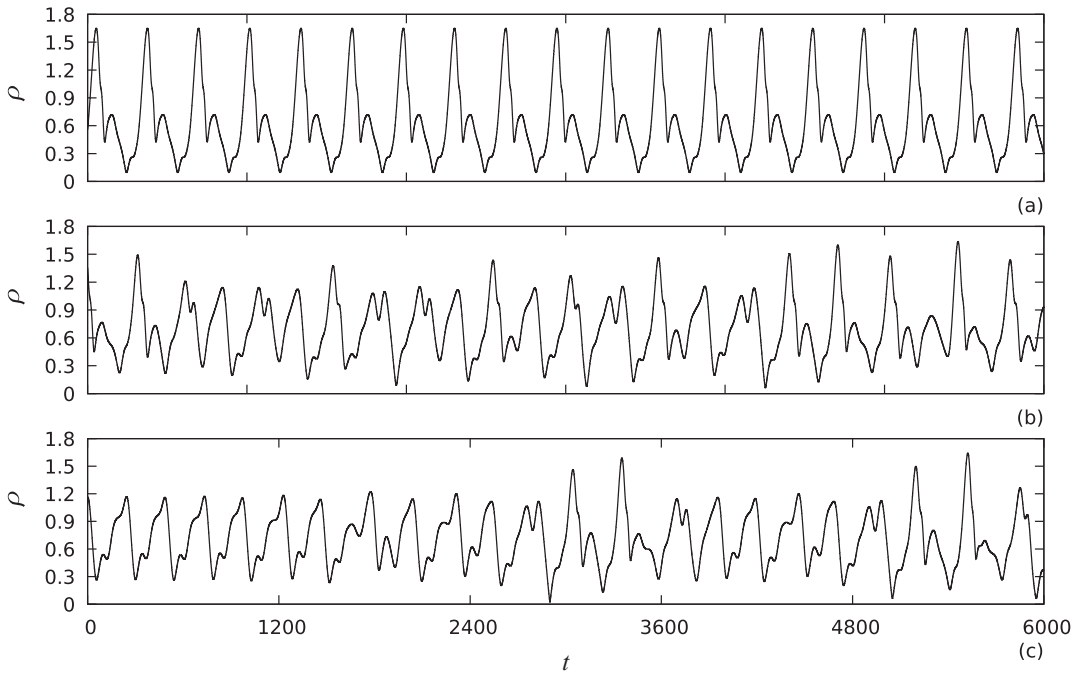


FIG. 1. The time series of $\rho(t)$ in the system (1) with $T = 1710$, $\alpha = 5$, $\Omega = -0.1962$, $P = 0.6$, and $\eta = 0.015$. (a) Periodic regime at $\tau = 60.5$. (b) Chaotic regime at $\tau = 63.5$. (c) Intermittent regime at $\tau = 65$.

$\Delta t = 0.05$ and $\tau = 60.5$, $\tau = 63.5$, and $\tau = 65$. The oscillation regime in Fig. 1(a) is periodic, and the regimes in Figs. 1(b) and 1(c) are chaotic. The transient process is excluded from the analysis to guarantee the dynamics on the attractor. At $\tau = 65$, the system exhibits intermittencylike behavior with long quasiregular epochs separated by epochs of irregular oscillations. Further throughout the paper we will call the regime with $\tau = 65$ as intermittent.

### A. Reconstruction of periodic regime

First, we apply the method to the system (1) reconstruction in a periodic regime. In Fig. 2, the periodic time series of all three dynamical variables of Eq. (1) with $\tau = 60.5$ ($\theta = 1210$) are shown in the background by a dashed black line. Note that we use only 10 000 points of time series for the system recovery; i.e., the upper time series in Fig. 2 is a short fragment of Fig. 1(a). The laser parameters $\tau$, $T$, $\alpha$, and $\Omega$ and the variable $\rho(t)$ are assumed to be known. Using the starting guesses $\tilde{P} = 0.65$, $\tilde{\eta} = 0.016\,75$, and $\tilde{F}_{\theta+1} = 0.023$, and the parameters $\tilde{\omega} = 7/\tau$, $\tilde{\varphi} = 0$, and $L = 4$ we calculate the time series of variables at the first step of the method application. These time series are presented in green (gray) in Fig. 2. Their shape is similar to the shape of the original time series, but the period of oscillations differs from the period of oscillations in the original model.

At the last step of the proposed technique, we obtain the time series shown in orange (light gray) in Fig. 2. For all variables, the orange (light gray) curves coincide closely with the dashed black curves. The original and reconstructed time series are practically indistinguishable in Fig. 2. Thus, the quality of time series reconstruction is very good. The parameters $P$ and $\eta$ are estimated as $\hat{P} = 0.600\,001$ and $\hat{\eta} = 0.015\,000\,4$, respectively, with the objective function value $S = 1.8 \times 10^{-9}$. The relative error of parameter reconstruction,

$$\delta = \frac{|P - \hat{P}|}{P} + \frac{|\eta - \hat{\eta}|}{\eta}, \tag{13}$$

takes the small value $\delta = 2.8 \times 10^{-5}$.

The quality of the system reconstruction depends on how successfully the starting guesses for unknown parameters are chosen. To test the method efficiency depending on the initial deviations of starting guesses from the true values of $P$ and $\eta$, we reconstruct the system (1) at different values of starting guesses $\tilde{P}$ and $\tilde{\eta}$, which differ from the true values by no more than 20%. The obtained results are presented in Fig. 3 for four different sets of values of $\tilde{F}_{\theta+1}$, $\tilde{\omega}$, and $\tilde{\varphi}$. The quality of the parameters $P$ and $\eta$ recovery is characterized by $\delta$ values, which are shown in different shades of gray in Fig. 3. The black squares in the $(\tilde{P}, \tilde{\eta})$ plane correspond to the starting guesses leading to the global minimum of the objective function (4) with $\delta \to 0$. If for the selected values of starting guesses, the error $\delta \leqslant 0.01$, then the corresponding square in the $(\tilde{P}, \tilde{\eta})$ plane is shaded in gray. Otherwise, the square is white. The square in the center of the $(\tilde{P}, \tilde{\eta})$ plane corresponds to the accurate choice of starting guesses at which the reconstruction is successful. It should be noted that for each set of starting guesses in Fig. 3, the reconstruction is carried out at various $L$ varying from 3 to 9. The results shown in Fig. 3 correspond to $L$ values, which give the smallest $S$ for each pair of $\tilde{P}$ and $\tilde{\eta}$ separately; i.e., the different gray squares in the same $(\tilde{P}, \tilde{\eta})$ plane can correspond to different $L$.

The bottom right corner of the $(\tilde{P}, \tilde{\eta})$ planes in Fig. 3 is occupied mainly by white squares. It can be explained by the fact that for $P$ and $\eta$ equal to $\tilde{P}$ and $\tilde{\eta}$ values in this part of the plane, system (1) exhibits an oscillation regime that is

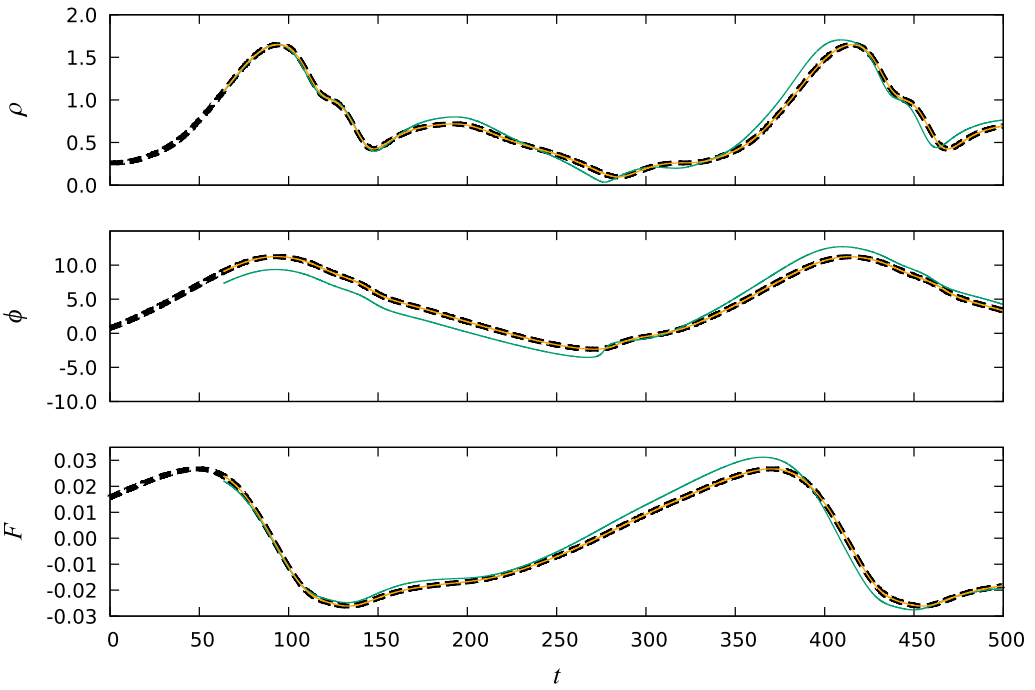


FIG. 2. Original periodic time series of dynamical variables of Eq. (1) with $\tau = 60.5$ (dashed black line), time series of variables at the first step of the algorithm [green (gray) line], and reconstructed time series at the last step of the algorithm [orange (light gray) line].

qualitatively different from the regime observed at $P$ and $\eta$ values taken from the center of the $(\tilde{P}, \tilde{\eta})$ plane. If the starting guesses $\tilde{P}$ and $\tilde{\eta}$ are chosen from the bottom right corner of Fig. 3, the algorithm typically does not converge to the regime observed at $P = 0.6$ and $\eta = 0.015$. Besides the four sets of $\tilde{F}_{\theta+1}$, $\tilde{\omega}$, and $\tilde{\varphi}$ values used for the construction of Fig. 3, there are a lot of other combinations of these parameters, which ensure good quality of reconstruction.

Each plot in Fig. 3 consists of $25 \times 25$ squares corresponding to different starting guesses $\tilde{P}$ and $\tilde{\eta}$. A more detailed variant of Fig. 3(b) consisting of $121 \times 121$ squares is presented in Fig. 4(a), in which the squares are shown in different shades of gray if the relative error $\delta \leqslant 0.01$. The portion of gray squares in Fig. 4(a) is 57% of the total number of squares. The black squares occupy 11% of the total number of squares.

Figure 4(a) shows in gray the starting guesses $\tilde{P}$ and $\tilde{\eta}$ that ensure high accuracy of the parameters $P$ and $\eta$ reconstruction with an error not exceeding 1%. To illustrate the error values larger than 0.01, we invert the colors and plot Fig. 4(b). The white squares in Fig. 4(b) correspond to the starting guesses leading to successful reconstruction of $P$ and $\eta$ with $\delta \leqslant 0.01$. Larger errors are shown in different shades of gray. The portion of gray squares in Fig. 4(b) is 43% of the total number of squares. The black squares, which correspond to $\delta \geqslant 1$, occupy about 1% of the total number of squares.

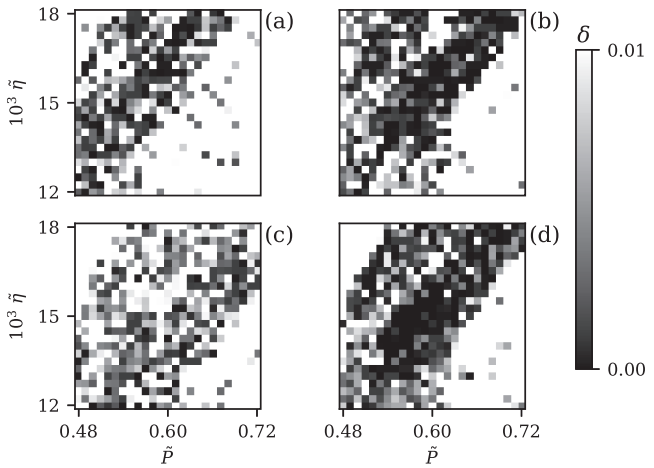


FIG. 3. Dependencies of error $\delta$ of parameters $P$ and $\eta$ reconstruction in the periodic regime with $\tau = 60.5$ on the choice of starting guesses $\tilde{P}$ and $\tilde{\eta}$. (a) $\tilde{F}_{\theta+1} = 0.022$, $\tilde{\omega} = 7/\tau$, and $\tilde{\varphi} = 0$. (b) $\tilde{F}_{\theta+1} = 0.023$, $\tilde{\omega} = 7/\tau$, and $\tilde{\varphi} = 0$. (c) $\tilde{F}_{\theta+1} = 0.024$, $\tilde{\omega} = 6/\tau$, and $\tilde{\varphi} = 1$. (d) $\tilde{F}_{\theta+1} = 0.025$, $\tilde{\omega} = 7.5/\tau$, and $\tilde{\varphi} = -1$.

### B. Reconstruction of chaotic regime

Chaotic regimes are typical for semiconductor lasers [50]. It has been shown that chaos can be used for chaos-based

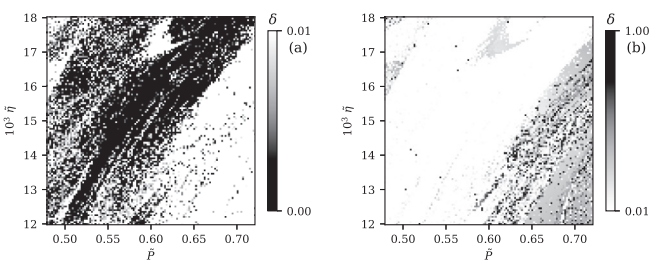


FIG. 4. Dependencies of error $\delta$ of parameters $P$ and $\eta$ reconstruction in the periodic regime with $\tau = 60.5$ on the choice of starting guesses $\tilde{P}$ and $\tilde{\eta}$. (a) Small errors with $\delta \leqslant 0.01$. (b) Large errors with $\delta > 0.01$.

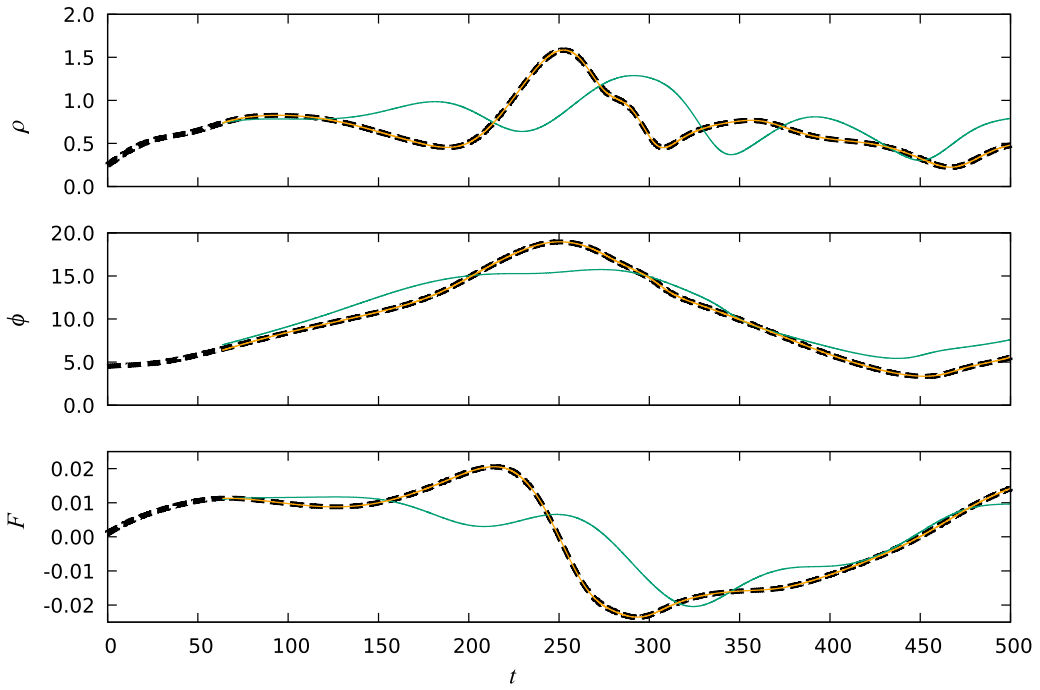


FIG. 5. Original chaotic time series of dynamical variables of Eq. (1) with $\tau = 63.5$ (dashed black line), time series of variables at the first step of the algorithm [green (gray) line], and reconstructed time series at the last step of the algorithm [orange (light gray) line].

secure communication systems [35–37,51–54] and generation of ultrafast random bit sequences [55,56]. We consider a chaotic regime, which occurs from the above-considered periodic regime under variation of $\tau$. Figure 5 shows with a dashed black line the chaotic time series of all three dynamical variables of Eq. (1) with $\tau = 63.5$. As in the case of periodic regime reconstruction, we use only 10 000 points of time series for the chaotic system recovery; i.e., the upper time series in Fig. 5 is a short fragment of Fig. 1(b).

With the starting guesses $\tilde{P} = 0.65$, $\tilde{\eta} = 0.01675$, and $\tilde{F}_{\theta+1} = 0.01$ and the method parameters $\tilde{\omega} = 3/\tau$, $\tilde{\varphi} = 4$, and $L = 3$, we calculate the time series of variables at the first step of the algorithm. These time series are shown in green (gray) in Fig. 5. At the last step of the algorithm, we obtain the time series shown in orange (light gray) in Fig. 5. For all variables, the reconstructed time series coincide closely with the original time series. The reconstructed parameters $P$ and $\eta$ take the values $\hat{P} = 0.600\,21$ and $\hat{\eta} = 0.015\,002$, respectively, while the objective function takes the value $S = 1.7 \times 10^{-7}$. The relative error $\delta = 4.8 \times 10^{-4}$ is an order of magnitude larger than in the case of periodic regime reconstruction, but is still small. The increase of $S$ and $\delta$ with respect to the periodic regime can be explained by the irregularity of the chaotic regime and the fact that the global minimum of the objective function (4) is achieved for smaller $L$, at which the approximation of initial conditions for $\phi(t)$ is worse than at larger $L$. However, the method convergence to the global minimum of the objective function is better for smaller $L$ values because of the smaller number of parameters of the objective function.

For both periodic and chaotic regimes, we consider relatively short time series, whose duration is much smaller than the Lyapunov time for the chaotic regime. As a result, the accuracy of time series reconstruction is similar for periodic and chaotic regimes, and Figs. 2 and 5 are also similar. In the case of chaotic regime reconstruction from long time series, the probability of getting into the global minimum of the objective function decreases.

The dependence of $\delta$ on the starting guesses $\tilde{P}$ and $\tilde{\eta}$ is presented in Fig. 6. If for the selected values of $\tilde{P}$ and $\tilde{\eta}$, the error $\delta > 0.01$, then the corresponding square in the $(\tilde{P}, \tilde{\eta})$ plane is shown in white. For $\delta \leqslant 0.01$, the squares are shown in different shades of gray. The portion of gray squares in Fig. 6 is 51% of the total number of squares. The black squares, which correspond to the starting guesses leading to the global minimum of the objective function (4) with very small $\delta$, occupy 20% of the total number of squares. The

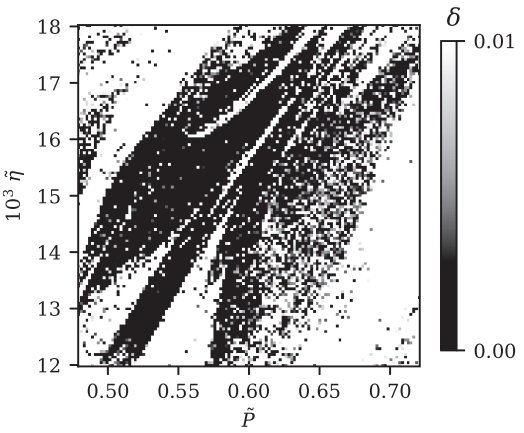


FIG. 6. Dependence of error $\delta$ of parameters $P$ and $\eta$ reconstruction in the chaotic regime with $\tau = 63.5$ on the choice of starting guesses $\tilde{P}$ and $\tilde{\eta}$.

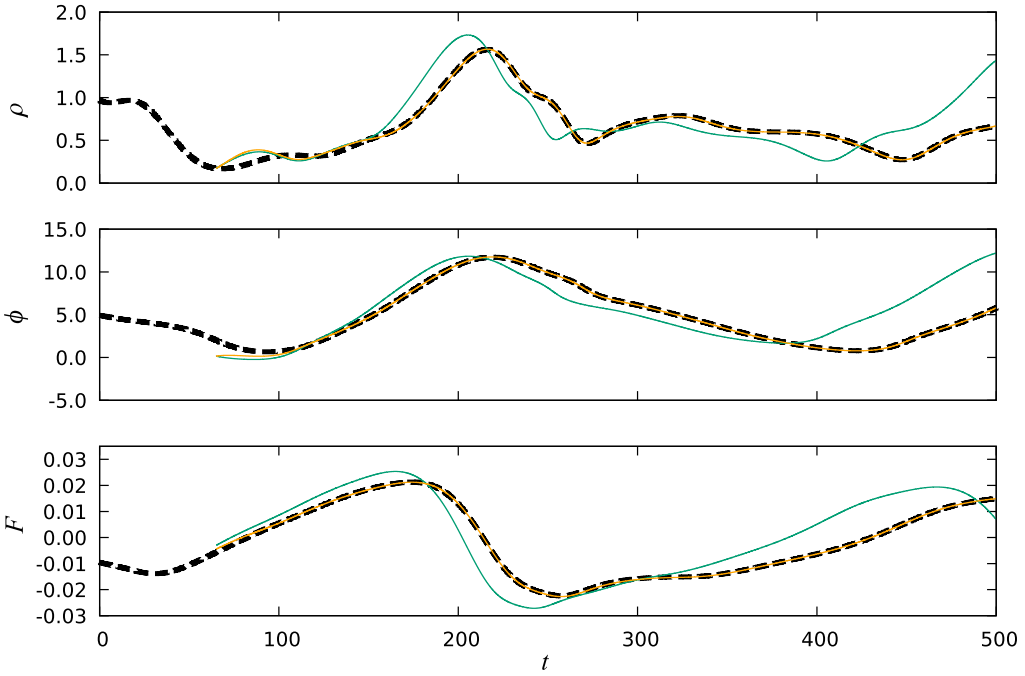


FIG. 7. Original intermittent time series of dynamical variables of Eq. (1) with $\tau = 65$ (dashed black line), time series of variables at the first step of the algorithm [green (gray) line], and reconstructed time series at the last step of the algorithm [orange (light gray) line].

portion of black squares in the chaotic regime (Fig. 6) is even larger than in the periodic regime [Fig. 4(a)].

### C. Reconstruction of intermittent regime

Finally, we apply the method for the system (1) reconstruction in a regime of intermittency observed at $\tau = 65$. In this regime, the epochs of almost periodic oscillations are interrupted by relatively short irregular transitions [Fig. 1(c)]. The reconstruction of such regime is more difficult, since small changes in the initial conditions for unobserved variables $F(t)$ and $\phi(t)$ can significantly change the frequency of switching between the epochs of quasiregular and irregular oscillations; i.e., the system dynamics is more sensitive to the values of $\tilde{F}_{\theta+1}$, $\tilde{\omega}$, and $\tilde{\varphi}$ than in the above-considered cases of periodic and chaotic oscillations.

TABLE I. Model parameters $\tau$, $T$, $\alpha$, $\Omega$, $P$, and $\eta$ and reconstructed parameters $\tilde{P}$ and $\tilde{\eta}$ for Figs. 2, 5, and 7 corresponding to periodic, chaotic, and intermittent regimes, respectively.

| | Regime | | |
|---|---|---|---|
| Parameter | Periodic | Chaotic | Intermittent |
| $\tau$ | 60.5 | 63.5 | 65 |
| $T$ | 1710 | 1710 | 1710 |
| $\alpha$ | 5 | 5 | 5 |
| $\Omega$ | –0.1962 | –0.1962 | –0.1962 |
| $P$ | 0.6 | 0.6 | 0.6 |
| $\eta$ | 0.015 | 0.015 | 0.015 |
| $\hat{P}$ | 0.600001 | 0.60021 | 0.60004 |
| $\hat{\eta}$ | 0.0150004 | 0.015002 | 0.014977 |

Using the starting guesses $\tilde{P} = 0.66$, $\tilde{\eta} = 0.016\,75$, and $\tilde{F}_{\theta+1} = -0.003$, and the method parameters $\tilde{\omega} = -5.5/\tau$, $\tilde{\varphi} = 5$, and $L = 8$, we calculate the time series of variables at the first step of the algorithm. These time series are presented in green (gray) in Fig. 7. At the last step of the algorithm, we obtain the time series shown in orange (light gray) in Fig. 7. The original and reconstructed time series are close to each other. The parameters $P$ and $\eta$ are estimated as $\hat{P} = 0.600\,04$ and $\hat{\eta} = 0.014\,977$, respectively, with the objective function value $S = 2.01 \times 10^{-4}$ and the relative error $\delta = 1.6 \times 10^{-3}$. The model and reconstructed parameters for periodic, chaotic, and intermittent regimes shown in Figs. 2, 5, and 7, respectively, are presented in Table I.

Figure 8 shows the dependence of the relative error of parameter reconstruction $\delta$ on the starting guesses $\tilde{P}$ and $\tilde{\eta}$.

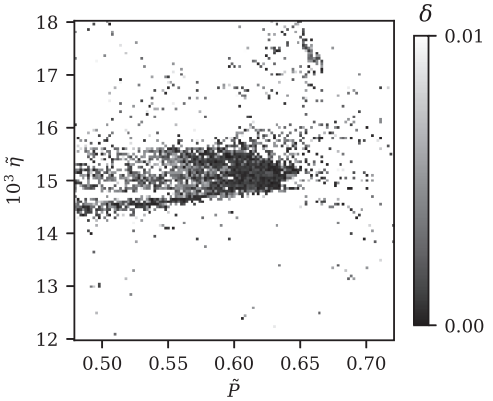


FIG. 8. Dependence of error $\delta$ of parameters $P$ and $\eta$ reconstruction in the regime of intermittency with $\tau = 65$ on the choice of starting guesses $\tilde{P}$ and $\tilde{\eta}$.

The portion of gray squares in Fig. 8 is 13% of the total number of squares. There are only 14 black squares (0.1%), starting from which the global minimum of the objective function is achieved. Thus, the probability of falling into a global minimum sharply decreased by two orders of magnitude in comparison with the cases of periodic and chaotic regimes, while the achievement of a local minimum became less probable in several times. To construct each of Figs. 4, 6, and 8 using GNU FORTRAN 8, LAPACK for least squares and OPENMP for parallel computing, it took us about 46 h with an Intel Core i5 4460 CPU.

## IV. CONCLUSION

We have proposed a method for the reconstruction of time-delayed feedback systems with unobserved variables from scalar time series. The method extends the initial condition approach to the case of a hidden variable having a time delay. The initial conditions for unobserved variables are considered as unknown parameters of the model, but instead of specifying starting guesses for a time-delayed hidden variable over the entire interval of the delay time, it is proposed to specify only a small number of starting guesses at the delay time and obtain the other initial conditions by interpolating the trajectory with a cubic spline. This approach allows one to reduce the number of starting guesses for a time-delayed hidden variable by several orders of magnitude. As the objective function of the method, the sum of squares of the distances between the points of the model time series and observed time series is used. The unknown model parameters and unobserved variables are reconstructed by minimizing the objective function. Thus, the considered approach can be used as a method for indirect measurement of unobserved variables.

The proposed method is applied to the reconstruction of the Lang-Kobayashi equations, which describe the dynamics of a single-mode semiconductor laser with external optical feedback. We have considered the case where only one of the three variables is observable and the other two variables of the model are hidden, including the hidden variable with a time delay. Such situation is typical for semiconductor lasers, since most experiments in laser physics are restricted to intensity measurements. Moreover, it is assumed that we do not know the laser parameters characterizing the pumping current and feedback strength, while the other model parameters including the delay time characterizing the optical feedback are known or can be reconstructed from time series of laser intensity using other methods [38–43]. Our approach allows one to solve a more challenging problem than the method [44] that accurately reconstructs the unobserved laser variables in the absence of delay-induced dynamics and under the assumptions that all laser parameters are known and all three dynamical variables are available for a limited period of time.

Despite the fact that the method often converges to a local minimum of the objective function, even in this case it can give a small error of the parameter reconstruction. We have studied the dependence of the quality of the model system reconstruction on the accuracy of assignment of starting guesses for unknown parameters and unobserved variables. It is shown that for periodic and chaotic regimes, the region of starting guesses for unknown parameters, which provides high quality of reconstruction, is larger than for the intermittent regime. The recovery of the parameters of semiconductor lasers gives a possibility of hidden message extraction for the communication schemes using chaotic signals of these systems. Since the reconstruction of the laser parameters in the intermittent regime is more difficult than in the chaotic regime, a laser-based communication system exploiting the intermittent regime can be more secure. On the other hand, the chaotic regime in Fig. 1(b) has a wider power spectrum than the intermittent regime in Fig. 1(c). Chaotic carrier signals with a broad power spectrum are known to be good candidates for laser-based secure communication [51].

Since the considered method gives access to the optical phase directly by measuring the optical intensity, it is promising for use in optical information processing [57]. The proposed method can be applied to the reconstruction of other time-delay systems with hidden variables from time series. It is possible to extend the method to the case of a larger number of hidden variables and unknown parameters in model equations. However, the success of reconstruction is less likely with an increase in the number of method parameters.

## ACKNOWLEDGMENT

This work was supported by the Russian Foundation for Basic Research, Grant No. 19-02-00071.

[1] Y. Bard, *Nonlinear Parameter Estimation* (Academic Press, New York, 1974).
[2] H. Kantz and T. Schreiber, *Nonlinear Time Series Analysis* (Cambridge University Press, Cambridge, 1997).
[3] B. P. Bezruchko and D. A. Smirnov, *Extracting Knowledge from Time Series: An Introduction to Nonlinear Empirical Modeling* (Springer, Berlin, 2010).
[4] H. Voss and J. Kurths, Phys. Lett. A **234**, 336 (1997).
[5] S. P. Ellner, B. E. Kendall, S. N. Wood, E. McCauley, and C. J. Briggs, Phys. D (Amsterdam, Neth.) **110**, 182 (1997).
[6] V. S. Udaltsov, L. Larger, J. P. Goedgebuer, A. Locquet, and D. S. Citrin, J. Opt. Technol. **72**, 373 (2005).
[7] L. Zunino, M. C. Soriano, I. Fischer, O. A. Rosso, and C. R. Mirasso, Phys. Rev. E **82**, 046212 (2010).
[8] A. C. Fowler and G. Kember, Phys. Lett. A **175**, 402 (1993).
[9] M. J. Bünner, Th. Meyer, A. Kittel, and J. Parisi, Phys. Rev. E **56**, 5083 (1997).
[10] Y.-C. Tian and F. Gao, Phys. D (Amsterdam, Neth.) **108**, 113 (1997).
[11] R. Hegger, M. J. Bünner, H. Kantz, and A. Giaquinta, Phys. Rev. Lett. **81**, 558 (1998).
[12] M. J. Bünner, M. Ciofini, A. Giaquinta, R. Hegger, H. Kantz, R. Meucci, and A. Politi, Eur. Phys. J. D **10**, 165 (2000).
[13] B. P. Bezruchko, A. S. Karavaev, V. I. Ponomarenko, and M. D. Prokhorov, Phys. Rev. E **64**, 056216 (2001).
[14] M. D. Prokhorov, V. I. Ponomarenko, A. S. Karavaev, and B. P. Bezruchko, Phys. D (Amsterdam, Neth.) **203**, 209 (2005).

[15] W. Horbelt, J. Timmer, and H. U. Voss, Phys. Lett. A **299**, 513 (2002).
[16] M. D. Prokhorov, V. I. Ponomarenko, and V. S. Khorev, Phys. Lett. A **377**, 3106 (2013).
[17] F. Sorrentino, Phys. Rev. E **81**, 066218 (2010).
[18] H. Ma, B. Xu, W. Lin, and J. Feng, Phys. Rev. E **82**, 066210 (2010).
[19] I. V. Sysoev, V. I. Ponomarenko, D. D. Kulminskiy, and M. D. Prokhorov, Phys. Rev. E **94**, 052207 (2016).
[20] S. Zhu and L. Gan, Phys. Rev. E **94**, 052210 (2016).
[21] X. H. Zhu, M. F. Cheng, L. Deng, X. X. Jiang, and D. M. Liu, Front. Optoelectron. **10**, 378 (2017).
[22] M. Siefert, Phys. Rev. E **76**, 026215 (2007).
[23] D. Yu, M. Frasca, and F. Liu, Phys. Rev. E **78**, 046209 (2008).
[24] V. I. Ponomarenko and M. D. Prokhorov, Phys. Rev. E **78**, 066207 (2008).
[25] M. D. Prokhorov and V. I. Ponomarenko, Phys. Rev. E **80**, 066206 (2009).
[26] R. Lang and K. Kobayashi, IEEE J. Quantum Electron. **16**, 347 (1980).
[27] P. M. Alsing, V. Kovanis, A. Gavrielides, and T. Erneux, Phys. Rev. A **53**, 4429 (1996).
[28] L. Junges, T. Pöschel, and J. A. C. Gallas, Eur. Phys. J. D **67**, 149 (2013).
[29] T. Heil, I. Fischer, W. Elsäßer, B. Krauskopf, K. Green, and A. Gavrielides, Phys. Rev. E **67**, 066214 (2003).
[30] A. Tabaka, K. Panajotov, I. Veretennicoff, and M. Sciamanna, Phys. Rev. E **70**, 036211 (2004).
[31] S. Behnia, K. Mabhouti, A. Jafari, and A. Akhshani, Optik **123**, 1555 (2012).
[32] E. V. Grigorieva, I. S. Kaschenko, and S. A. Kaschenko, Nonlinear Phenom. Complex Syst. **15**, 403 (2012).
[33] S. Heiligenthal, T. Jüngling, O. D'Huys, D. A. Arroyo-Almanza, M. C. Soriano, I. Fischer, I. Kanter, and W. Kinzel, Phys. Rev. E **88**, 012902 (2013).
[34] R. Vicente, J. Daudén, P. Colet, and R. Toral, IEEE J. Quantum Electron. **41**, 541 (2005).
[35] S. Sivaprakasam and K. A. Shore, Opt. Lett. **24**, 1200 (2000).
[36] I. Fischer, Y. Liu, and P. Davis, Phys. Rev. A **62**, 011801(R) (2000).
[37] A. Locquet, in *Handbook of Information and Communication Security*, edited by P. Stavroulakis and M. Stamp (Springer, Berlin, 2010), p. 451.
[38] V. I. Ponomarenko, M. D. Prokhorov, and I. V. Koryukin, Tech. Phys. Lett. **31**, 939 (2005).
[39] D. Rontani, A. Locquet, M. Sciamanna, D. S. Citrin, and S. Ortin, IEEE J. Quantum Electron. **45**, 879 (2009).
[40] J.-G. Wu, Z.-M. Wu, G.-Q. Xia, and G.-Y. Feng, Opt. Express **20**, 1741 (2012).
[41] R. M. Nguimdo, G. Verschaffelt, J. Danckaert, and G. Van der Sande, Opt. Lett. **37**, 2541 (2012).
[42] X. Porte, O. D'Huys, T. Jüngling, D. Brunner, M. C. Soriano, and I. Fischer, Phys. Rev. E **90**, 052911 (2014).
[43] V. S. Khorev, M. D. Prokhorov, and V. I. Ponomarenko, Tech. Phys. Lett. **42**, 146 (2016).
[44] A. Cunillera, M. C. Soriano, and I. Fischer, Chaos **29**, 113113 (2019).
[45] E. Baake, M. Baake, H. G. Bock, and K. M. Briggs, Phys. Rev. A **45**, 5524 (1992).
[46] B. P. Bezruchko, D. A. Smirnov, and I. V. Sysoev, Chaos, Solitons Fractals **29**, 82 (2006).
[47] O. Strebel, Chaos, Solitons Fractals **57**, 93 (2013).
[48] V. Gorodetskyi and M. Osadchuk, Int. J. Dyn. Control **3**, 341 (2015).
[49] I. V. Sysoev, V. I. Ponomarenko, and M. D. Prokhorov, Izv. VUZ. Appl. Nonlinear Dynamics **25**, 84 (2017).
[50] J. Ohtsubo, *Semiconductor Lasers, Stability, Instability and Chaos* (Springer, Berlin, 2006).
[51] A. Argyris, D. Syvridis, L. Larger, V. Annovazzi-Lodi, P. Colet, I. Fischer, J. Garcia-Ojalvo, C. R. Mirasso, L. Pesquera, and K. A. Shore, Nature **438**, 343 (2005).
[52] C. P. Xue, N. Jiang, Y. X. Lv, C. Wang, G. L. Li, S. Q. Lin, and K. Qiu, Opt. Lett. **41**, 3690 (2016).
[53] C. Wang, Y. F. Ji, H. X. Wang, and L. Bai, IEEE Photonics J. **10**, 7203415 (2018).
[54] L. F. Liu and Q. Liu, IET Optoelectron. **13**, 94 (2019).
[55] A. Uchida, K. Amano, M. Inoue, K. Hirano, S. Naito, H. Someya, I. Oowada, T. Kurashige, M. Shiki, S. Yoshimori, K. Yoshimura, and P. Davis, Nat. Photonics **2**, 728 (2008).
[56] I. Reidler, Y. Aviad, M. Rosenbluh, and I. Kanter, Phys. Rev. Lett. **103**, 024102 (2009).
[57] G. Van der Sande, D. Brunner, and M. C. Soriano, Nanophotonics **6**, 561 (2017).